

Amplitude Variations in Pulsating Red Giants. II. Some Systematics

John R. Percy

Department of Astronomy and Astrophysics, and Dunlap Institute of Astronomy and Astrophysics, University of Toronto, Toronto, ON M5S 3H4, Canada; john.percy@utoronto.ca

Jennifer Laing

Department of Astronomy and Astrophysics, University of Toronto, Toronto, ON M5S 3H4, Canada; jen.laing@mail.utoronto.ca

Received September 22, 2017; revised October 16, 2017; accepted October 19, 2017

Abstract In order to extend our previous studies of the unexplained phenomenon of cyclic amplitude variations in pulsating red giants, we have used the AAVSO time-series analysis package *VSTAR* to analyze long-term AAVSO visual observations of 50 such stars, mostly Mira stars. The relative amount of the variation, typically a factor of 1.5, and the time scale of the variation, typically 20–35 pulsation periods, are not significantly different in longer-period, shorter-period, and carbon stars in our sample, and they also occur in stars whose period is changing secularly, perhaps due to a thermal pulse. The time scale of the variations is similar to that in smaller-amplitude SR variables, but the *relative* amount of the variation appears to be larger in smaller-amplitude stars, and is therefore more conspicuous. The cause of the amplitude variations remains unclear, though they may be due to rotational modulation of a star whose pulsating surface is dominated by the effects of large convective cells.

1. Introduction

Percy and Abachi (2013) showed that, in almost all pulsating red giants (PRGs), the pulsation *amplitude* varied by a factor of up to 10, on a time scale of 20–40 pulsation periods. The authors were initially concerned that the variation might be an artifact of wavelet analysis, but it can be confirmed by Fourier analysis of individual sections of the dataset. Similar amplitude variations were found in pulsating red supergiants (Percy and Khatu 2014) and yellow supergiants (Percy and Kim 2014). There were already sporadic reports in the literature of amplitude variations in PRGs (e.g. Templeton *et al.* 2008; Price and Klingenberg 2005), but these stars tended to be the rare few which also showed large changes in period, and which may be undergoing thermal pulses (Uttenthaler *et al.* 2011). Furthermore, it is well known that stars such as Mira do not repeat exactly from cycle to cycle. Percy and Abachi (2013), however, was the first *systematic* study of this phenomenon. Since these amplitude variations remain unexplained, we have examined the behavior of more PRGs to investigate some of the systematics of this phenomenon.

We have analyzed samples of *large-amplitude* PRGs, mostly Mira stars, in each of four groups: A: 17 shorter-period stars; B: 20 longer-period stars; C: 15 carbon stars; D: 8 stars with significant secular period changes (Templeton *et al.* 2005). The stars in groups A, B, and C were drawn randomly from among the 547 studied by Templeton *et al.* (2005) and which did not show significant secular period changes. As did Templeton *et al.* (2005), we used visual observations from the American Association of Variable Star Observers (AAVSO) International Database. We did not analyze stars for which the data were sparse, or had significant gaps. Note that Templeton *et al.* (2005) specifically studied Mira variables, which, by definition, have full ranges greater than 2.5 in visual light—an arbitrary limit.

The purposes of this paper are: (1) to present our analyses of these 50 PRGs, and (2) to remind the astronomical community,

once again, that the amplitude variations in PRGs require an explanation.

2. Data and analysis

We analyzed visual observations from the AAVSO International Database (AID; Kafka 2017) using the AAVSO’s *VSTAR* software package (Benn 2013). It includes both a Fourier and wavelet analysis routine; we used primarily the latter. The wavelet analysis uses the Weighted Wavelet Z-Transform (WWZ) method (Foster 1996). The “wavelet” scans along the dataset, estimating the most likely value of the period and amplitude at each point in time, resulting in graphs which show the best-fit period and amplitude versus time.

For each star, we noted the Modified Julian Date MJD(1) after which the data were suitable for analysis—not sparse, no significant gaps. The datasets are typically a century long so, for these mostly-Mira stars, there are typically at least a hundred pulsation cycles in the dataset. From the WWZ wavelet plots, we determined the maximum (Amx), minimum (Amn), and average (\bar{A}) amplitude, the number of cycles N of amplitude increase and decrease, and the average length L of these cycles. See Percy and Abachi (2013) for a discussion of these quantities and their uncertainties; N and therefore L can be quite uncertain because the cycles are irregular, and few in number, especially if they are long. This is doubly true for the few stars in which the length of the dataset is shorter than average. The maximum and minimum amplitudes are also uncertain since they are determined over a limited interval of time.

We then calculated the ratio of L in days to the pulsation period P in days, the ratio of maximum to minimum amplitude, the difference ΔA between the maximum and minimum amplitude, and the ratio of this to the average amplitude \bar{A} . The periods were taken from the VSX catalog, and rounded off; the periods of stars like these “wander” by several percent, due to random cycle-to-cycle fluctuations. All this information is listed in Tables 1–4. In the “Notes” column, the symbols are as

Table 1. Pulsation properties of shorter-period PRGs.

<i>Name</i>	<i>P(d)</i>	<i>MJD(1)</i>	<i>N</i>	<i>L/P</i>	<i>Amn</i>	<i>Amx</i>	<i>Amx/Amn</i>	\dot{A}	ΔA	$\Delta A/\dot{A}$	<i>Note</i>
T And	281	16000	8	18	2.38	2.78	1.17	2.60	0.40	0.15	s
V And	256	20000	5	29	2.17	2.63	1.21	2.40	0.46	0.19	s
UW And	237	39000	1	80	1.68	2.21	1.32	2.00	0.53	0.27	d
YZ And	207	40000	3	28	2.00	2.51	1.26	2.25	0.51	0.23	—
S Car	151	20000	10	25	1.03	1.46	1.42	1.25	0.43	0.34	—
U Cas	277	20000	6	22	2.50	3.50	1.40	3.30	1.00	0.30	s
SS Cas	141	27500	5	43	1.28	1.78	1.39	1.55	0.50	0.32	—
Z Cet	184	25000	7	25	2.00	2.45	1.23	2.25	0.45	0.20	—
T Phe	282	20000	3	44	2.00	3.10	1.55	2.50	1.10	0.44	d
W Psc	188	40000	4	23	1.75	2.15	1.23	1.95	0.40	0.21	s
RZ Sco	160	25000	5	41	0.80	1.70	2.13	1.30	0.90	0.69	d*
T Scl	205	32000	2	63	1.40	2.40	1.71	1.70	1.00	0.59	d
V Scl	296	30000	3	31	2.05	2.85	1.39	2.50	0.80	0.32	g
X Scl	265	33000	6	15	1.60	2.03	1.27	1.80	0.43	0.24	—
S Tuc	242	23000	6	24	2.35	2.85	1.21	2.65	0.50	0.39	s
U Tuc	262	20000	6	24	2.35	2.85	1.21	2.70	0.50	0.19	g
R Vir	149	20000	8	31	1.56	2.25	1.44	1.95	0.69	0.35	—

Table 2. Pulsation properties of longer-period PRGs.

<i>Star</i>	<i>P(d)</i>	<i>MJD(1)</i>	<i>N</i>	<i>L/P</i>	<i>Amn</i>	<i>Amx</i>	<i>Amx/Amn</i>	\dot{A}	ΔA	$\Delta A/\dot{A}$	<i>Note</i>
R And	410	20000	7	13	3.19	3.60	1.13	3.38	0.41	0.12	g
X And	343	16000	6	20	1.90	3.00	1.58	2.60	1.10	0.42	d
RR And	331	20000	5	22	2.68	3.18	1.19	3.00	0.50	0.17	s
RW And	430	15000	4	25	2.45	3.50	1.43	3.10	1.05	0.34	—
SV And	313	15500	6	22	2.15	2.80	1.30	2.45	0.65	0.27	—
TU And	313	37000	2	33	1.85	2.30	1.24	2.15	0.45	0.21	—
R Aqr	386	28000	4	19	1.80	2.20	1.22	1.95	0.40	0.21	—
R Car	310	20000	6	20	2.23	2.60	1.17	2.40	0.38	0.16	—
R Cas	430	15000	5	20	2.60	2.98	1.14	2.73	0.38	0.14	—
T Cas	445	20000	2	42	1.15	1.97	1.71	1.75	0.82	0.47	d
Y Cas	414	14500	4	26	1.80	2.28	1.27	2.05	0.48	0.23	g
RV Cas	332	20000	9	12	2.50	3.25	1.30	2.90	0.75	0.26	s
TY Cas	645	40000	1	27	2.28	3.20	1.40	2.90	0.92	0.32	s
Y Cep	333	15000	5	25	1.50	3.10	2.07	2.80	1.60	0.57	d
o Cet	332	20000	7	16	2.60	3.05	1.17	2.80	0.45	0.16	—
S Cet	321	20000	5	23	2.30	2.87	1.25	2.70	0.57	0.21	—
W Cet	352	32500	2	36	2.35	3.30	1.40	2.80	0.95	0.34	—
R Cyg	434	15000	5	19	2.73	2.98	1.09	2.83	0.25	0.09	—
R Hor	408	25000	5	16	2.95	3.67	1.24	3.45	0.72	0.21	g
Z Peg	320	20000	2	59	1.90	2.40	1.26	2.20	0.50	0.23	d

Table 3. pulsation properties of some carbon PRGs.

<i>Star</i>	<i>P(d)</i>	<i>MJD(1)</i>	<i>N</i>	<i>L/P</i>	<i>Amn</i>	<i>Amx</i>	<i>Amx/Amn</i>	\dot{A}	ΔA	$\Delta A/\dot{A}$	<i>Note</i>
AZ Aur	415	40000	2.5	17	1.35	1.75	1.30	1.65	0.40	0.24	s
W Cas	406	20000	3.5	26	1.18	1.45	1.23	1.27	0.27	0.21	d
X Cas	423	20000	5	17	0.70	0.93	1.32	0.80	0.23	0.28	—
RV Cen	457	20000	3.5	23	0.83	1.23	1.48	1.03	0.40	0.39	g
V CrB	358	20000	6	17	1.36	1.75	1.29	1.50	0.39	0.26	—
U Cyg	463	20000	4	20	1.23	1.55	1.26	1.45	0.32	0.22	—
T Dra	422	20000	3	30	0.60	1.55	2.58	1.30	0.95	0.73	gd
R For	386	33000	5	12	1.17	1.53	1.31	1.35	0.36	0.27	d
VX Gem	379	40000	1.5	31	1.65	2.15	1.30	1.85	0.50	0.27	gd
ZZ Gem	315	40000	2.5	22	0.83	1.22	1.47	1.07	0.39	0.36	g
R Lep	445	20000	4	21	0.75	1.27	1.69	1.05	0.52	0.50	d*
T Lyn	406	28000	4	18	1.18	1.53	1.30	1.40	0.35	0.25	—
V Oph	295	25000	5	22	1.03	1.30	1.27	1.13	0.28	0.24	—
RU Vir	434	20000	4.5	19	1.25	1.78	1.42	1.40	0.53	0.38	—
R Vol	453	20000	4	20	0.95	1.65	1.74	1.40	0.70	0.50	gd

Table 4. pulsation properties of some PRGs with rapidly-changing periods.

Star	$P(d)$	$MJD(1)$	N	L/P	Amn	Amx	Amx/Amn	\bar{A}	ΔA	$\Delta A/\bar{A}$	Note
R Aql	311	20000	4	30	1.83	2.58	1.41	2.20	0.75	0.34	—
R Cen	502	20000	1	75	0.60	1.70	2.83	1.40	1.10	0.79	d*
V Del	543	20000	2	34	2.58	3.30	1.28	2.85	0.72	0.25	s
W Dra	291	20000	4	32	1.62	2.58	1.59	2.20	0.96	0.44	—
R Hya	414	20000	3	30	1.40	2.25	1.61	1.70	0.85	0.50	*
R Leo	319	20000	5	23	1.60	2.05	1.28	1.87	0.45	0.24	—
S Scl	367	20000	4.5	23	2.52	3.13	1.24	2.85	0.61	0.21	g
Z Tau	446	20000	3	28	1.45	2.78	1.92	1.90	1.33	0.70	ds*

follows: “s”—the data were sparse in places; “g”—there were one or more gaps in the data (but not enough to interfere with the analysis); “d”—the star is discordant in one or more graphs mentioned below, but there were no reasons to doubt the data or analysis; asterisk (*)—see Note in section 3.2. Note that the amplitudes that we determine and list are “half-amplitudes” rather than the full ranges, i.e., they are the coefficient of the sine function which fit to the data.

3. Results

We plotted L/P , Amx/Amn , and $\Delta A/\bar{A}$ against period for each of the four groups of stars A, B, C, and D. There was no substantial trend in any case, except as noted below (Figures 1–3). We therefore determined the mean M , the standard error SE , and the standard error of the mean SEM , for each of the three quantities, for each of the four groups. (The mean M is more commonly called the average; the standard error SE is a measure of the scatter of the values around the mean; and the standard error of the mean SEM is a measure of the uncertainty of the mean, given the scatter of the values, and the number thereof.) These are given in Table 5. We also flagged any outliers in the graphs, and re-examined the data and analysis. If there was anything requiring comment, that comment is given in section 3.2.

In stars which are undergoing large, secular period changes, possibly as a result of a thermal pulse, the size and length of the amplitude variation cycles is marginally larger, but this may be partly due to the difficulty of separating the cyclic and secular variations. Note that cyclic variations in amplitude are present during the secular ones in these stars.

We also found that, for the shorter-period stars, \bar{A} increased with increasing period (Figure 4), but this is a well-known

Table 5. Properties of the amplitude variation in four samples of PRGs.

Property	SP	LP	C	CP
$M(\Delta A/\bar{A})$	0.31	0.26	0.34	0.43
$SE(\Delta A/\bar{A})$	0.15	0.12	0.14	0.22
$SEM(\Delta A/\bar{A})$	0.036	0.028	0.037	0.076
hline				
$M(Am x/Amn)$	1.38	1.33	1.46	1.65
$SE(Am x/Amn)$	0.24	0.23	0.35	0.53
$SEM(Am x/Amn)$	0.058	0.052	0.089	0.188
hline				
$M(L/P)$	33	25	21	34
$SE(L/P)$	17	11	5	17
$SEM(L/P)$	4.1	2.5	1.3	6

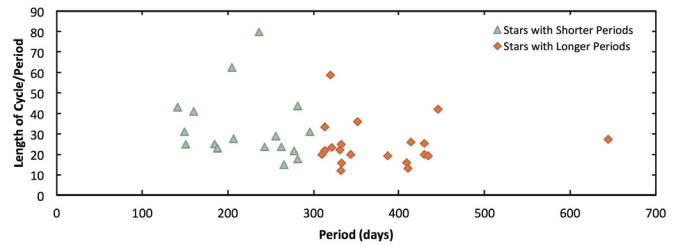


Figure 1. The lengths of the cycles of amplitude increase and decrease, in units of the pulsation period, as a function of pulsation period. At most, there is a slight downward trend, which may be partly due to the fact that the cycles may be more difficult to detect in shorter-period, smaller-amplitude stars.

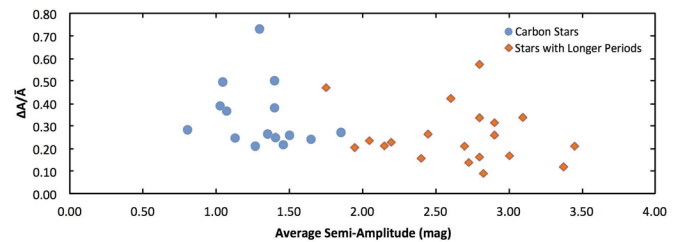


Figure 2. The variation in visual amplitude, relative to the average visual amplitude, as a function of average visual amplitude, for carbon stars (blue filled circles) and non-carbon stars (red filled diamonds). The difference is not significant to the 3σ level (Table 5).

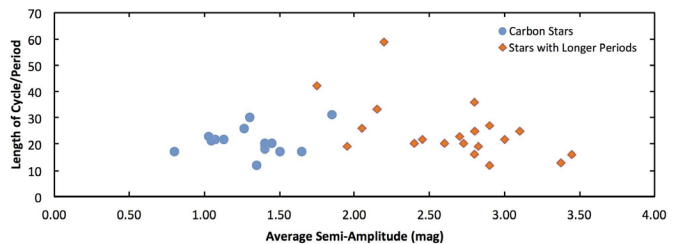


Figure 3. The lengths of the cycles of amplitude increase and decrease, in units of the pulsation period, as a function of average visual amplitude, for carbon stars (blue filled circles) and non-carbon stars (red filled diamonds). There is no trend. The visual amplitudes of the carbon stars are systematically smaller, as is well-known.

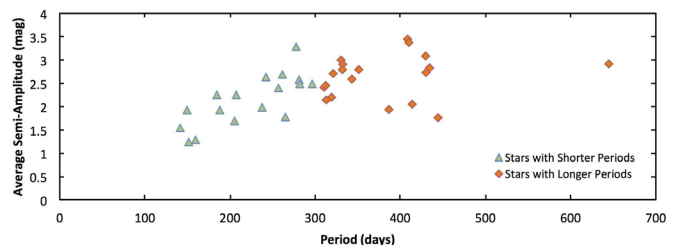


Figure 4. The average visual pulsation amplitude as a function of pulsation period, for shorter- period and longer-period Miras. The amplitude increases with period, up to about 300 days (this is a continuation of a well-known trend), and then levels off.

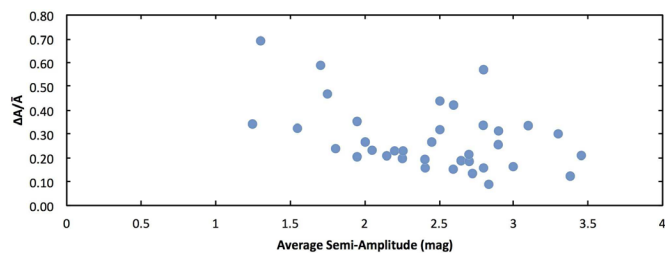


Figure 5. The variation in visual amplitude, relative to the average visual amplitude, as a function of average visual amplitude. There is a downward trend. This trend is consistent with the results of Percy and Abachi (2013), who found values of typically 0.5 to 2.0 for stars with average amplitudes of 1.0 down to 0.1.

correlation. The very shortest-period PRGs have amplitudes of only hundredths of a magnitude. There was no trend in amplitude for the longer-period stars.

The *relative* amount of variation in amplitude is slightly larger in shorter-period, smaller-amplitude stars (Figure 5). This is consistent with the results of Percy and Abachi (2013), as discussed in section 4.

The \bar{A} for the carbon stars are systematically lower than for the oxygen stars (Figures 2 and 3). Again, this is well-known; in the oxygen stars, the visual amplitude is amplified by the temperature sensitivity of TiO bands, which are not present in carbon stars. Note also that the carbon stars have longer periods, since they are in a larger, cooler, and more highly evolved state.

3.1. Stars with secular amplitude variations

Although our main interest was in the cyclic variations in pulsation amplitude, the secular variations in amplitude are also of interest, though they have already been studied and discussed by other authors, as mentioned in the Introduction. We performed a quick wavelet analysis of the 547 Miras in Templeton *et al.*'s (2005) paper, to identify stars in which *secular* amplitude variations might dominate the cyclic ones. Of the 21 stars whose period varied secularly at the three-sigma level or greater, four (T UMi, LX Cyg, R Cen, and RU Sco) seemed to show such secular amplitude variations. There were no other stars in Templeton *et al.*'s (2005) sample which showed *strong* secular variations. Note that, in each case, cyclic amplitude variations were superimposed on the secular ones.

3.2. Notes on individual stars

This section includes notes on two kinds of stars: the ones for which the data or analysis required comments, and ones which appear to be outliers in some of the graphs that we have plotted.

R Cen This star has a secular decrease in amplitude, and period, so it is not surprising that the star is discordant in some of the relationships; see also Templeton *et al.* (2005).

T Dra This star has unusually large cyclic variations in amplitude.

R Lep This star has unusual large variations in mean magnitude.

RZ Sco This star, with a relatively short period, has a secular change in period, but only at the 3σ level (Templeton *et al.* 2005).

Z Tau This star is exceptional in that it is an S-type star.

Also, its light curve shows non-sinusoidal variations, and flat minima suggestive that the variable may have a faint companion star. Indeed, SIMBAD lists two faint stars within 5 arc seconds of Z Tau. This star is discussed by Templeton *et al.* (2005).

4. Discussion

Percy and Abachi (2013) obtained a median value of $L/P = 44$ for 28 monoperoic smaller-amplitude PRGs. They calculated the median, in part because there were a few stars with very large values of L/P . We have reanalyzed those stars, and realized that Percy and Abachi (2013) adopted a more conservative definition for amplitude variations. Figure 6 shows an example of this: for the smaller-amplitude PRG RY Cam, Percy and Abachi (2013) estimated $N = 1.5$ whereas, based on our subsequent experience, we would estimate $N = 6.7$. Based on our reanalysis, the L/P values are now strongly clustered between 20 and 30, with a mean of 26.6. This is consistent with the values which we obtained for shorter- and longer-period PRGs. Figure 7 shows the light curve of RY Cam on which Figure 6 is based.

The values of $\Delta A/\bar{A}$, obtained by Percy and Abachi (2013), for smaller-amplitude (1.0 down to 0.1) variables, are typically about 0.5 to 2.0. This is consistent with the trend shown in Figure 5. The amplitude variations are relatively larger and more conspicuous in small-amplitude stars.

Templeton *et al.* (2008) call attention to three other PRGs with variable amplitudes. The amplitude variations in RT Hya are the largest (0.1 to 1.0) and are cyclic ($L/P=40$). The amplitude variations in W Tau are almost as large (0.1 to 0.6) and are also cyclic ($L/P=24$). Those in Y Per are less extreme (0.3 to 0.9) and also cyclic ($L/P = 29$). These three stars therefore behave similarly to PRGs in our sample.

There are therefore at least three unexplained phenomena in the pulsation of PRGs: (1) random, cycle-to-cycle fluctuations which cause the period to “wander”; (2) “long secondary periods,” 5 to 10 times the pulsation period; and now (3) cyclic variations in pulsation amplitudes, on timescales of 20 to 30 pulsation periods. PRGs have large outer convective envelopes. Stothers and Leung (1971) proposed that the long secondary periods represented the overturning time of giant convective cells in the outer envelope, and Stothers (2010) amplified this conclusion. Random convective cells may well explain the random cycle-to-cycle period fluctuations, as well. The amplitude variations might then be due to rotational modulation, since the rotation periods of PRGs are significantly longer than the long secondary periods according to Olivier and Wood (2003).

5. Conclusions

Significant cyclic amplitude variations occur in all of our sample of 50 mostly-Mira stars. The relative amount of the variation (typically $A_{mx}/A_{mn} = 1.5$) and the time scale of the variation (typically 20–35 times the pulsation period) are not significantly different in the shorter-period and longer-period stars, and in the carbon stars. The time scales are consistent with those found by Percy and Abachi (2013) in a sample of mostly smaller-amplitude SR variables, but the *relative* amplitude

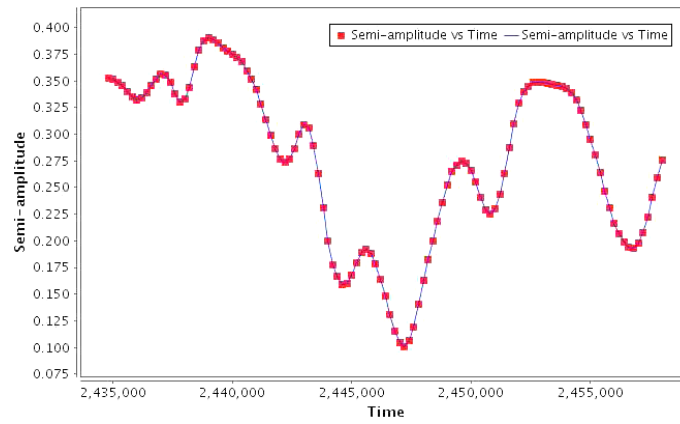


Figure 6. Semi-amplitude versus time for RY Cam, a smaller-amplitude PRG. Percy and Abachi (2013) estimated N conservatively at 1.5 but, based on our subsequent experience, we would estimate $N = 6.7$. This figure therefore illustrates both the significant amplitude variation, and the somewhat subjective estimate of N and therefore L .

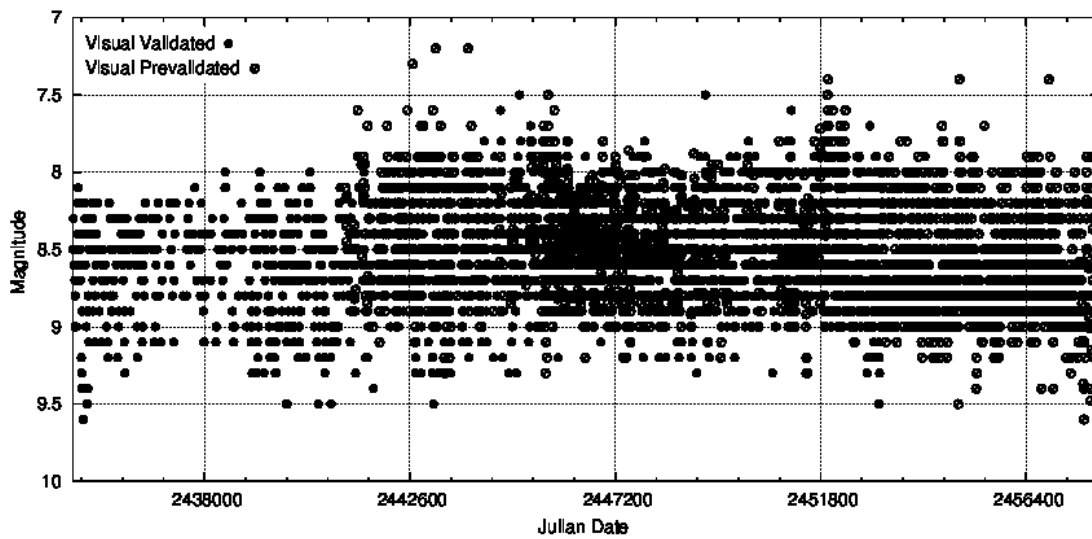


Figure 7. The visual light curve of RY Cam on which Figure 6 is based, taken from the AAVSO International Database. It begins where the data become dense and continuous enough for wavelet analysis.

variations are larger in the smaller-amplitude stars. As was previously known, the average amplitudes increase with period for the shorter-period stars, and the carbon stars have smaller visual amplitudes than the oxygen stars.

6. Acknowledgements

We thank the AAVSO observers who made the observations on which this project is based, the AAVSO staff who archived them and made them publicly available, and the developers of the *vSTAR* package which we used for analysis. This paper is based, in part, on a short summer research project by undergraduate astronomy and physics student co-author JL. We acknowledge and thank the University of Toronto Work-Study Program for existing, and for financial support. This project made use of the SIMBAD database, maintained in Strasbourg, France.

References

- Benn, D. 2013, *vSTAR* data analysis software (<http://www.aavso.org/vstar-overview>).
- Foster, G. 1996, *Astron. J.*, **112**, 1709.
- Kafka, S. 2017, variable star observations from the AAVSO International Database (<https://www.aavso.org/aavso-international-database>).
- Olivier, E. A., and Wood, P. R. 2003, *Astrophys. J.*, **584**, 1035.
- Percy, J. R., and Abachi, R. 2013, *J. Amer. Assoc. Var. Star Obs.*, **41**, 193.
- Percy, J. R., and Khatu, V. C. 2014, *J. Amer. Assoc. Var. Star Obs.*, **42**, 1.
- Percy, J. R., and Kim, R. Y. H. 2014, *J. Amer. Assoc. Var. Star Obs.*, **42**, 267.
- Price, A., and Klingenberg, G. 2005, *J. Amer. Assoc. Var. Star Obs.*, **34**, 23.
- Stothers, R. B. 2010, *Astrophys. J.*, **725**, 1170.
- Stothers, R. B., and Leung, K. C. 1971, *Astron. Astrophys.*, **10**, 290.
- Templeton, M. R., Mattei, J. A., and Willson, L. A. 2005, *Astron. J.*, **130**, 776.
- Templeton, M. R., Willson, L. A., and Foster, G. 2008, *J. Amer. Assoc. Var. Star Obs.*, **36**, 1.
- Uttenhaller, S., et al. 2011, *Astron. Astrophys.*, **531**, A88.